Thermodynamic Performance Assessment of a Bio-gasification Based Small-scale Combined Cogeneration Plant Employing Indirectly Heated Gas Turbine

P. Mondal[*], S. Ghosh[**‡]

[*]PhD Scholar, Department of Mechanical Engineering, IIEST, Shibpur, W. B.-711103, India
[*] Associate Professor, Department of Mechanical Engineering, IIEST, Shibpur, W. B.-711103, India

‡Corresponding Author; Ph + 91 33 2668 4561/62/63 Ext 279 Fax: + 91 33 2668 2916, sudipghosh.becollege@gmail.com

Received: 10.12.2014 Accepted:13.02.2015

Abstract- Thermodynamic model development of biomass gasification based indirectly heated combined cogeneration plant and its simulated performance is reported in this present study. Saw dust is considered as biomass feed, which undergoes gasification in a downdraft gasifier and the producer gas is combusted in a combustor-heat exchanger duplex (CHX) unit. The CHX unit heats up air for a 100 kWe Gas Turbine (GT) and the exhaust heat of CHX unit is utilized in generating bottoming steam turbine work output and utility steam. The performance of the plant is assessed over a wide range pressure ratio (rp) and turbine inlet temperature (TIT) for the GT block, as well as, by varying the steam turbine inlet pressure and temperature along with the outlet gas side temperature of the economizer. For the base case configuration (rp= 4 and TIT=1000 deg C) the plant gives an overall electrical efficiency of about 41% and, at the same time, produces utility steam at a rate of about 180 kg/hr. Its cogeneration performance, expressed in terms of fuel energy saving ratio (FESR), is found to optimize at particular values of topping cycle pressure ratio for different TITs. The study also includes discussion on the sizing of the major plant components. Further, a Second law analysis of the plant concludes that maximum exergy destruction takes place at the gasifier, followed by the CHX unit, together accounting for nearly 40% of the fuel exergy input.

Keywords: Bio-gasification; Indirectly heated; Combined cogeneration; Fuel energy saving ratio; exergy

1. Introduction

Biomass based power generation is getting increased importance worldwide in overcoming the energy scarcity problems and environmental issues [1]. Wide ranges of biomass gasifier-gas engine assembly are commercially available for decentralized power generation. However, these systems suffer from low overall efficiency (~20-25 %) and extensive gas cleaning and cooling requirement [2]. The internal combustion (IC) engines are very sensitive to the presence of tar, particles and moisture in the producer gas and so additional gas cleaning and drying systems are required after the gasifiers which ultimately affect the operation and maintenance cost [3]. The energy researchers are paying attention into the integration of bio-gasification with gas turbine (GT)-steam turbine (ST) combined cycle plant, which can improve the overall electrical efficiency substantially [4]. The Worlds' first bio-gasification based combined cycle power plant was operated during 1996 in Varnamo, Sweden with an overall efficiency of 32%. The operation of the plant was stopped due to high operation and maintenance cost [5] as extensive gas cleaning and cooling were required for the combustor and gas turbine.

Solid biomass is thermo-chemically converted into gaseous products through its gasification in oxygen deficient environment. The main components of the gas are CH4, H2, CO, CO2, H2O and N2. Different types of tars are also produced during gasification as by-product [6]. The producer gas needs to be extremely clean to avoid erosion, corrosion of and particulate deposition on the gas turbine blades and blockage of the fuel injectors. Also, since the calorific value of the product gas is low compared to natural gas,

modification of the combustor is also essential for the usage of producer gas in conventional GT [7].

The gas cleaning and cooling complexities along with the modification requirement of combustor and rotor balding can be avoided by implementing a combustor-heat exchanger duplex (CHX) unit instead of conventional gas combustor used in a GT cycle [8]. The CHX unit burns the producer gas and heats up the air for GT. The exhaust from the GT is utilized in generating superheated steam for the bottoming Rankine cycle. Datta et al [7] carried out an energetic and exergetic performance analyses of an externally fired gas turbine cycle, wherein it is seen that the cycle reaches a maximum efficiency at particular value of topping cycle pressure ratio, depending on turbine inlet temperature (TIT) and cold end temperature difference (CETD) of the heat exchanger.

Zanial and Al-attab [9] had experimentally studied the performance of the heat exchanger used in an EGFT cycle. It is observed that the heat exchanger is capable of producing about 7000C TIT at 63% average effectiveness. Soltani et al. [10] had also carried out the similar analysis of an externally fired combined cycle (EFCC) plant. Most of the studies suggest that the design of the heat exchanger, used in the CHX unit is the most critical parameter from operational point of view.

In this paper, thermodynamic modeling and performance assessment of a combined cogeneration plant is reported. The issue of the sizing of the major plant components has also been discussed. The gas turbine block of the modeled plant is designed considering a fixed output of 100 kWe, while the power and utility steam generation from the bottoming HRSG vary with varying pressure ratio and TIT of the GT. Saw dust is used as fuel feed for the plant and the gasifier is of downdraft type. Variation in overall efficiency, work output, electrical specific biomass consumption (ESBC) and fuel energy savings ratio (FESR) are analyzed over a wide range pressure ratio (2-12) and turbine inlet temperature (900, 1000 and 1100 deg C) for the GT block, as well as, by varying the steam turbine inlet pressure (4-16 bar) and temperature (200-365 deg C) along with the outlet gas side temperature of the economizer (120-200 deg C).

Exergetic performance of the plant, identifying the major exergy destroying components has also been attempted in this paper. The model development and thermal performance assessment have been carried out using Cycle-Tempo software [11].

2. Proposed Plant Configuration

"Fig. 1" shows the schematic diagram of the conceptualized biomass based indirectly heated combined cogeneration plant. Solid biomass (saw dust) is fed to a downdraft gasifier (block 6) to convert it into producer gas, in the presence of atmospheric air, in sub-stoichiometric condition. The hot producer gas is directly allowed to feed into the combustion chamber (block 7), where it gets combusted in the presence of recirculated gas turbine (GT) exhaust air.

Flue gas, generated during the combustion process, enters the shell side of a high pressure high temperature (tube side) air heater (block 8). Block 7 and block 8 together called as combustor-heat exchanger duplex (CHX) unit, which heats up the working medium (air) of the topping GT cycle. Atmospheric air after passing through the compressor (block 9) enters the CHX unit and gets heated up. The hot and compressed air then expands in the gas turbine (block 10) to atmospheric pressure and enters the combustion chamber of the CHX unit. An electric generator is coupled with the gas turbine rotor to produce electricity.

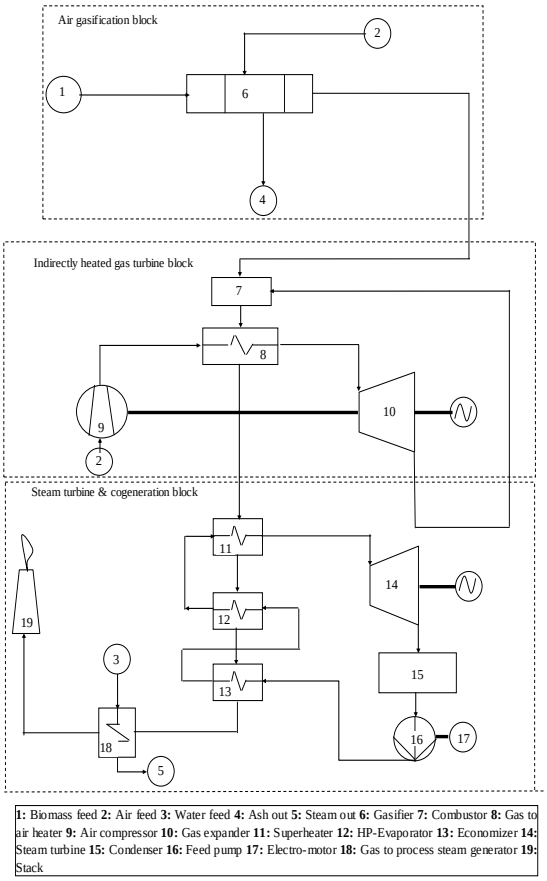

Figure 1. Schematic of the proposed plant

The heat exhausted from the CHX unit is recovered through a heat recovery steam generator (HRSG), consisting of four sub-units; superheater (block 11), HP evaporator (block 12), economizer (block 13) and LP evaporator (block 18). The superheater, HP evaporator, economizer, steam turbine (block 14), condenser (block 15) and feed pump (block 16) constitute the bottoming steam power cycle. The pump is driven by an electric motor (block 17). The exhaust heat of HRSG unit passes through the LP evaporator and

produces utility steam for heating purpose. The plant exhaust is exposed to the atmosphere through stack (block 19).

3. Model Development

Thermodynamic First Law and Second Law analyses have been carried out for the plant, varying certain design and performance parameters. The model development and thermal performance assessment have been carried out using Cycle-Tempo software. In Cycle-Tempo, different components models are available in the component library from which necessary components can be picked and connected to represent a process or a cycle.
The following sections describe the assumptions and applicable thermodynamic relations for the relevant processes and components.

3.1. First Law Analysis

The following assumptions are made for the analyses [7, 10]:

- The biomass gasifier is fixed bed downdraft type and chemical equilibrium model is considered.

- Ultimate analysis of biomass is presented in Table 1. Moisture content is 16 %.The equivalence ratio for the gasification is 0.35 and gasification temperature is 680^0C.

- Tar formation is negligible and not considered here.Ash is represented by SiO_2 for this model.

- No extraneous heat loss occurs in the plant components and in the ducts.

- Pressure drop across the gasifier is considered to be 2.13 kPa, while that for combustion chamber is 0.5% of the inlet pressure. Pressure drop across the cold side of the heat exchanger is 3% and hot side is 1.5% of the corresponding inlet pressure. No pressure loss occurs in the gas path and in the steam path is considered for the bottoming cycle.

- The bottoming cycle consists of non reheat Rankine cycle operating at 10 bar and 400^0C. The condenser pressure is 0.1 bar.

- The isentropic efficiencies of air compressor and GT are 87% and 89% respectively, while the same for bottoming ST is 90%.

- The process steam block operates at 1.5 bar. For the HRSG, minimum pinch point temperature difference is set to 10^0C. The stack temperature is 120^0C.

3.1.1 Gasification Unit

The dry biomass feedstock can be expressed by the generalized molecular formulae $CH_PO_QN_R$. The subscripts P, Q and R are determined using the ultimate analysis of biomass, presented in "Table 1".

Table 1. Ultimate analysis of fuel used [1].

Composition	Mass Percentage on Dry Basis (%)
C	52.28
H	5.2
N	0.47
O	40.85
Ash	1.2

The generalized global gasification reaction is presented as:

$$CH_PO_QN_R + bH_2O + X_0(O_2 + 3.76N_2) \rightarrow \rightarrow X_1H_2 + X_2CO + X_3CO_2 + X_4H_2O + + X_5CH_4 + X_6N_2 \quad (1)$$

Where X_1, X_2, X_3, X_4, X_5 and X_6 are the number of moles of the respective gas species. X_0 is the moles of O_2 in gasification air and b is the moisture associated with every mole of the biomass.

The syngas composition is calculated using mass balance for carbon, hydrogen, oxygen Eq. 1 and considering equilibrium for methanation and water-gas shift reactions Eq. 2. The product gas composition and gasifier outlet temperature is dependent on the "equivalence ratio" of the gasifier. The equilibrium constants of the said equations are dependent on the gasification temperature (T_{gasi}).

$$CO + H_2O \rightarrow CO_2 + H_2$$
$$C + 2H_2 \rightarrow CH_4 \quad (2)$$

The efficiency of the gasification process is calculated as follows:

$$\eta_{gasi} = \frac{m_{p.g} LHV_{p.g}}{m_b LHV_b} \quad (3)$$

3.1.2 Compressor and Gas/air Turbine Unit

Compressor (block 9) work requirement per mol of admitted air is expressed as:

$$w_C = c_{p,air}(T_{c,o} - T_{c,i}) \quad (4)$$

Where, compressor outlet temperature (Tc,o) is calculated using the compressor pressure ratio (r_p) and isentropic efficiency of the compressor.
Gas turbine (block 10) work output per mol of admitted air is expressed as:

$$w_{GT} = c_{p,air}(T_{GT,i} - T_{GT,o}) \quad (5)$$

Where, turbine outlet temperature (T_{GT},o) is calculated using the turbine pressure ratio (r_p) and isentropic efficiency of the turbine.

3.1.3 Combustor-Heat Exchanger Duplex (CHX) Unit

Hot producer gas gets combusted in the combustion chamber of the CHX unit (block 7), in the presence of recirculated GT exhaust air. The combustion equation can be represented as follows:

$$X_1H_2 + X_2CO + X_3CO_2 + X_4H_2O + X_5CH_4 + X_6N_2 + X_0'(O_2 + 3.76N_2) \rightarrow X_7CO_2 + X_8H_2O + X_9O_2 + (X_6 + 3.76X_0')N_2 \quad (6)$$

Where X_7, X_8 and X_9 are the number of moles of CO_2, H_2O and O_2 present in the flue gas X_0' denotes mol of O_2 entering the combustion chamber. The post combustion temperature is calculated using energy balance equation of the streams and considering the adiabatic condition as:

$$\sum_j X_j(\overline{h_{fj}^o} + \int_{T_{Gasi,o}}^{T_{pc}} c_{p_j}\Delta T)_{pg} + \sum_k X_k(\overline{h_{fk}^o} + \int_{T_{GT,o}}^{T_{pc}} c_{p,air}\Delta T)_{air} = \sum_m X_m(\overline{h_{fm}^o} + \int_{T_{Gasi,o}}^{T_{pc}} c_{fm}\Delta T)_{fg} \quad (7)$$

Where *Xj*, *Xk* and *Xm* represent the numbers of moles of the *j*th, *k*th and *m*th component in the producer gas, air and flue gas, h and c_p represents the enthalpy of formation and specific heat.

The products of combustion (that occurs in the combustor section of CHX unit), exchange heat with the compressed air within the tubular heat exchanger (block 8) section of the CHX unit, thus, transferring heat to the topping cycle working fluid, i.e. air. The heat balance equation for the heat exchanger is:

$$4.76X_0'c_{p,air}(T_{GT,i} - T_{C,o}) = X_{fg}c_{p,fg}(T_{CHX,i} - T_{CHX,o}) \quad (8)$$

Where X_{fg} is the total mole flow rate of the flue gas flowing through the heat exchanger and calculated as:

$$\sum_m X_m = X_{fg} = X_7 + X_8 + X_9 + (X_6 + 3.76X_0') \quad (9)$$

3.1.4 Steam Turbine Unit and Process Steam Generator

The exhaust of the CHX unit is recovered through a HRSG, consisting three sub-units viz. superheater (block 11), HP evaporator (block 12), economizer (block 13) and LP evaporator (block 18). The power steam generation rate is calculated from the combined energy balance of economizer and evaporator and the steam rate, so calculated, decides the temperature drop of GT exhaust air that superheats the power steam before being recirculated to the CHX unit.

$$X_{fg}c_{p,fg}(T_{CHX,o} - T_{PSG,i}) = X_s(\Delta h_{EV} + \Delta h_{ECO} + \Delta h_{SH}) \quad (10)$$

Where, X_S denotes the number of moles of power steam entering the ST.

The steam turbine electrical output is expressed as:

$$W_{ST} = X_s(h_{ST,i} - h_{ST,o})\eta_G' \quad (11)$$

The feed pump is driven by an electromotor through external power source and pump work is neglected.

The CHX exhaust is further utilized for saturated steam generation purpose at 1.5 bar. The process steam generation rate is calculated as:

$$X_{fg}c_{p,fg}(T_{PSG,i} - T_{Stack,i}) = X_{ps}(h_f - h_g) = Q_U \quad (12)$$

Where, Q_U represents the utility heat and X_{PS} is the moles of process steam.

The energetic performance of the plant is accessed considering three important parameters viz. Electrical Efficiency, ESBC and FESR along with the sizing of the major plant components.

Net work output from the topping cycle is expressed as:

$$W_{net.GT} = 4.76X_0'(w_{GT} - w_C)\eta_G \quad (13)$$

And combined work from the plant is expressed as:

$$W_{CC} = W_{net.GT} + W_{ST} \quad (14)$$

The overall electrical efficiency of the combined cycle plant is expressed as:

$$\eta_{e.CC} = \frac{W_{CC}}{m_b\, LHV_b} \quad (15)$$

Where, m_b represents the biomass consumption rate equivalent to one formula mol of biomass feed to the plant.

Electrical specific biomass consumption-ESBC (kg/kWh) is expressed as:

$$ESBC = \frac{3600m_b}{W_{CC}} \quad (16)$$

Although several approaches have been proposed, considering first law to evaluate the performance of a cogeneration plant, the fuel energy savings ratio (FESR) calculation method is significant for indicating the savings in fuel of a combined power and heating plant instead of separate power and heating plants[12, 13].

The fuel saving for the plant is expressed considering against a pair of bio-gasification based separate heating and power plants as:

$$\Delta F = (\frac{W_{CC}}{\eta_{e,ref}} + \frac{Q_U}{\eta_{b,ref}}) - m_b\, LHV_b \quad (17)$$

The reference efficiency values are set to be 25 percent and 80 percent for the individual power and heat plants respectively. The FESR is given by:

$$FESR = \frac{\Delta F}{(\frac{W_{CC}}{\eta_{e,ref}} + \frac{Q_U}{\eta_{b,ref}})} \quad (18)$$

3.2 Second Law Analysis

Exergy analysis of the plant components is based on stream exergy as well as heat and work interactions applicable for the individual plant components. Stream exergy is calculated based on pressure, temperature and chemical composition of any stream either at the inlet or at the outlet of a component. Physical exergy is defined as the maximum useful work obtainable by system as it passes from its initial state to 'restricted dead state'. Chemical exergy is the maximum useful work obtainable by system as it passes from 'restricted dead state' to 'dead state' and is in complete equilibrium with reference environment. The reference environment is Po=1.01325 bar and To=25^{0}C [14].

Specific thermo-mechanical exergy at any state of a cycle is calculated using a generalized equation as:

$$e_i = (h_i - h_o) - T_o(s_i - s_o) \quad (19)$$

Where, *i* represents the state point at which exergy is evaluated and *o* represents the reference environment.

Now,

$$h_i - h_o = \int_{T_o}^{T_i} c_p dT$$
$$s_i - s_o = \int_{T_o}^{T_i} c_p \frac{dT}{T} - \bar{R}\ln\frac{P_i}{P_o} \quad (20)$$

The specific fuel exergy is given by [7]:

$$e_{fuel} = LHV_{biomass}\beta \quad (21)$$

The factor (β) in the above equation is expressed as [7]:

$$\beta = \frac{1.044 + 0.0160\frac{H}{C} - 0.34493\frac{O}{C}(1 + 0.0531\frac{H}{C})}{1 - 0.4124\frac{O}{C}} \quad (22)$$

Exergy input to the plant can be expressed as:

$$e_{plant,i} = e_{fuel} + w.e_{H_2O} + 4.76(X_0 + X_0^{'})e_{air} \quad (23)$$

Exergy loss for a plant component is evaluated with respect to the fuel exergy input for the plant. This helps in identifying the components where major exergy destruction occurs. Also the exergetic efficiency of a plant component can be defined as:

$$n_{exergetic} = e_{out} \Big/ e_{in} \quad (24)$$

Where, ex_{in} is the sum of exergies of the streams entering into a component and the work inputs w_{in}, if any [14] and thus:

$$e_{in} = \Sigma(e_i)_{in} + \Sigma(w_i)_{in} \quad (25)$$

Subscript i represents any stream of flow or work. Similarly, exergy coming out ex_{out} from the control volume is given by:

$$e_{out} = \Sigma(e_i)_{out} + \Sigma(w_i)_{out} \quad (26)$$

The exergy loss is the difference between the incoming exergy and outgoing exergy of streams i.e. (ex_{in}-ex_{out}). "Table 2" shows the exergy destruction and exergetic efficiency of the individual plant components.

4. Results and Discussions

Energetic and exergetic performance of the conceptualized plant along with some discussion on the sizing of the major plant components are reported in this section. The performance of the gasifier, considering saw dust as biomass feed is presented in "Table 3". The producer gas composition, obtained from the model is compared with the commercially available gasifier (Ankur Gasifier [2]).

The biomass based combined cogeneration plant is designed considering a base case (r_p=4 and TIT=1000^{0}C) and the performance of the plant is shown in Table 4 at the base case. It is seen form "Table 4" that the plant is capable of producing both electrical and utility steam with an overall electrical efficiency of about 40% and process steam generation rate of 180kg/hr. Also, at base case the value of FESR is about 41% with ESBC of 0.54 kg/kWh.

The variation in overall electrical efficiency with topping cycle pressure ratio at different gas turbine inlet temperatures is shown in "Fig. 2".

Table 2. Exergy destruction and exergetic efficiency of the plant components [7, 11]

Component	Exergy destruction	Exergetic efficiency
Gasifier	$\bar{e}^{ch}_{sawdust} + 4.76X_0\bar{e}_{air} + w\bar{e}_{moisture} - X_{pg}(\bar{e}^{ch}_{pg} + \bar{e}_{pg})$	$\frac{X_{pg}(\bar{e}^{ch}_{pg} + \bar{e}_{pg})}{\bar{e}^{ch}_{sawdust} + 4.76X_0\bar{e}_{air} + w\bar{e}_{moisture}}$
Compressor	$4.76X'_0\Delta\bar{e}_C + W_C$	$\frac{W_C}{4.76X'_0\Delta\bar{e}_C}$
Combustion chamber	$4.76X_0\bar{e}_{air,GT,o} + X_{pg}(\bar{e}^{ch}_{pg} + \bar{e}_{pg}) - X_{fg}\bar{e}_{fg,o}$	$\frac{X_{fg}\bar{e}_{fg,o}}{4.76X_0\bar{e}_{air,GT,o} + X_{pg}(\bar{e}^{ch}_{pg} + \bar{e}_{pg})}$
Heat exchanger	$X_{fg}\Delta\bar{e}_{HX} + 4.76X'_0\Delta\bar{e}_{air,HX}$	$\frac{4.76X'_0\Delta\bar{e}_{air,HX}}{X_{fg}\Delta\bar{e}_{HX}}$
Gas turbine	$4.76X'_0\Delta\bar{e}_{GT} - W_{GT}$	$\frac{W_{GT}}{4.76X'_0\Delta\bar{e}_{GT}}$
Steam turbine	$X_s\Delta\bar{e}_{ST} - W_{ST}$	$\frac{W_{ST}}{X_s\Delta\bar{e}_{ST}}$
HRSG	$X_{fg}\Delta\bar{e}_{HRSG} + X_s\Delta\bar{e}_{HRSG}$	$\frac{X_s\Delta\bar{e}_{HRSG}}{X_{fg}\Delta\bar{e}_{HRSG}}$
Pump	$X_s\Delta\bar{e}_{ST} + W_P$	$\frac{X_s\Delta\bar{e}_{ST}}{W_P}$
Condenser	$X_{cw}\Delta\bar{e}_{Cond} + X_s\Delta\bar{e}_{Cond}$	$\frac{X_s\Delta\bar{e}_{Cond}}{X_{cw}\Delta\bar{e}_{Cond}}$
Utility steam generator	$X_{fg}\Delta\bar{e}_{USG} + X_{ps}\Delta\bar{e}_{USG}$	$\frac{X_{ps}\Delta\bar{e}_{USG}}{X_{fg}\Delta\bar{e}_{USG}}$

Table 3. Performance of the gasifier model and experimental result of Ankur gasifier (experimental).

Gas Composition (% mole fraction)	Present Model	Ankur Gasifier
H_2	21.44	18±3
CO	22.14	19±3
CO_2	10.57	10±3
CH_4	0.54	Upto 3
N_2	39.09	45-50
H_2O	5.76	------
Air-fuel Ratio	1.6	1.5-1.8
LHV (MJ/kg)	5.04	4.40-5.40
Gasification efficiency	%	82

Table 4. Base case performance of the plant.

Parameter	Unit	Value
GT Output	kWe	100
ST Output	kWe	33.51
Overall Electrical Efficiency	%	40.61
Utility Steam Generation Rate	kg/h	180.5
Required Air flow through Topping GT Cycle	kg/s	0.53
FESR	%	41.01
ESBC	kg/kWh	0.54

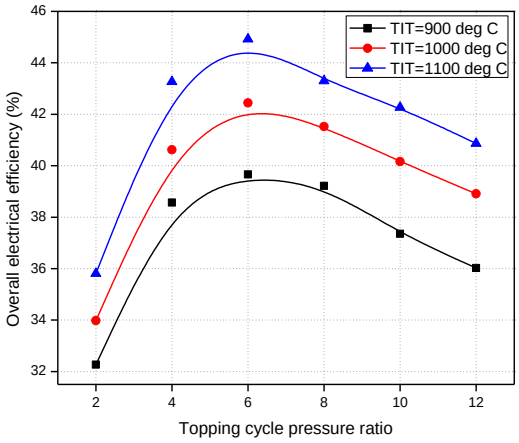

Figure 2. Variation in overall efficiency of the plant with topping cycle pressure ratio

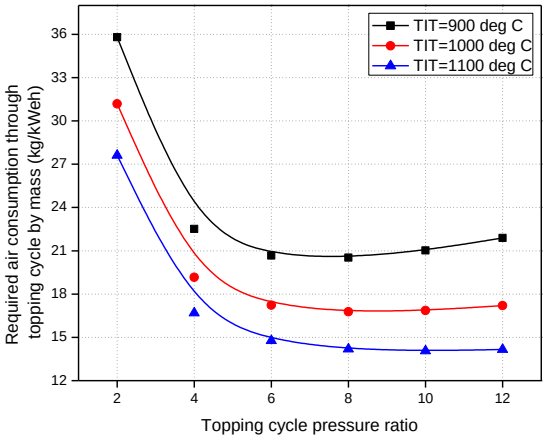

Figure 3. Variation in required air consumption through topping cycle by mass with topping cycle pressure ratio

The performance of the plant is found to be influenced greatly by the variations in topping cycle pressure ratio and gas turbine inlet temperature. Overall electrical efficiency of the plant initially increases with increase in topping cycle pressure ratio and then decreases for a fixed TIT as shown in "Fig. 2". This is due to fact that the value of specific work output from the topping cycle is maximized at certain values of pressure ratio and then decreases with further increase in pressure ratio. Now, the net work output form the topping cycle is considered to be fixed for the present study. Hence the required air consumption (by mass) of the topping cycle initially decreases, gets minimized at certain pressure ratio and then increases with increase in pressure ratio, as shown in "Fig. 3". This ultimately results in the required ESBC to decrease initially and then to increase with increase in pressure ratio as shown in "Fig. 4". Hence the overall electrical efficiency of the plant initially increases, gets maximized and then decreases with increase in pressure ratio. "Fig. 2" also indicates that higher TIT results in higher efficiency at individual pressure ratios. This is also due to the fact that ESBC decreases with increase in plant output as shown in "Fig 4" and GT-ST work ratio increases with increase in the same as shown in "Fig. 5".The maximum efficiency point shifts slightly towards the right end of the graph as the TIT increases.

It is also evident from "Fig. 3" that the air consumption rate decreases with increase in TIT at a particular pressure ratio as the specific work output from the topping cycle is higher at higher TITs. Also, for a fixed value of topping cycle pressure ratio, the required ESBC decreases as the TIT increases. This is because of the required air flow through topping GT cycle decreases with increase in TITs thus ultimately affecting in the required heat input to decrease with increase in the same.

"Fig. 5" shows the variation in GT-ST work ratio of the plant with topping cycle pressure ratio at different TITs. The graph clearly shows that the work ratio initially increases, gets maximized and then decreases with increase in pressure ratio at individual TITs. This is due to the fact that required ESBC of the plant decreases with increase in TIT. This results in bottoming ST output to decrease with increase in TIT which ultimately results in work ratio to increase with increase in GT output.

The variation in fuel energy savings ratio (FESR) with topping GT cycle pressure ratio is shown in "Fig. 6". The graph follows a trend opposite to that of "Fig. 4" and this is obvious and can be clearly understood from Eq. (17) and Eq. (18).

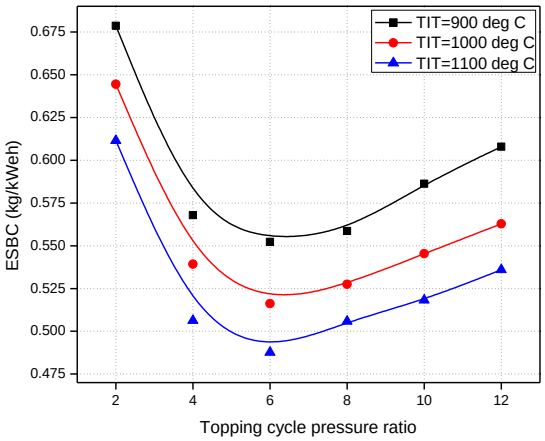

Figure 4. Variation in ESBC with topping cycle pressure ratio

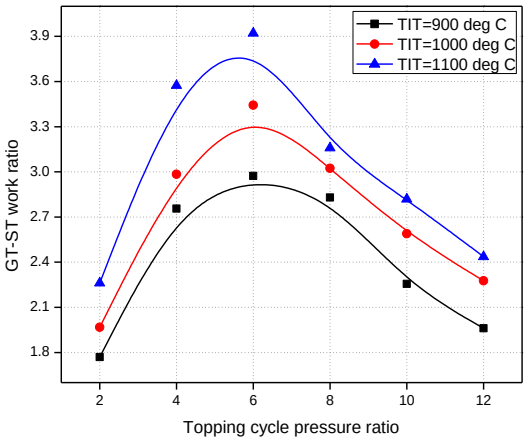

Figure 5. Variation in GT-ST work ratio with topping cycle pressure ratio

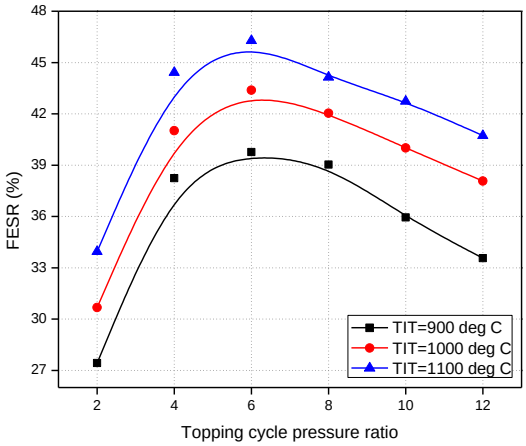

Figure 6. Variation in FESR with topping cycle pressure ratio

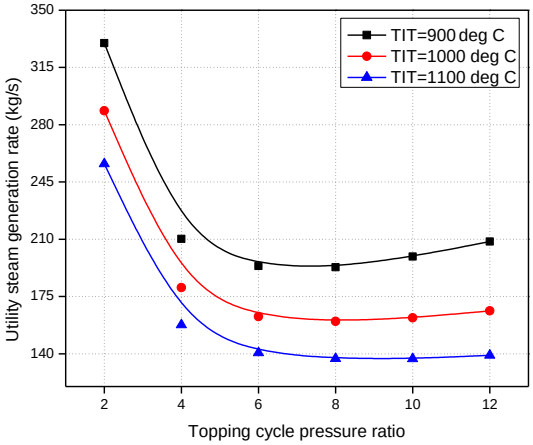

Figure 7. Variation in utility steam generation rate with topping cycle pressure ratio

"Fig. 7" shows the variation in utility steam generation rate with GT cycle pressure ratio. Utility steam generation initially decreases, gets minimized and then increases with increase in pressure ratio. Also the steam generation rate is higher at lower TITs at a particular value of topping cycle pressure ratio due to the fact that at lower TITs the required air consumption as well as biomass consumption increases, leading to more heat release in the LP evaporator. This results in increased process steam generation rate. The graph follows the same trend as followed by "Fig. 3" and "Fig. 4" and this is obvious. The required topping cycle air flow rate also influences the size of the gas/air turbine. For the low pressure end of the turbine the size is usually determined by the specific air consumption by mass while that for high pressure end is determined by the specific air consumption by volume [7].

From "Fig. 3" it is clear that the size of the bottom end of the turbine is minimized at pressure ratio 6.3 and TIT of 1100 deg C. "Fig. 8" shows the variation in required air consumption by volume with topping cycle pressure ratio to predict the size of high pressure end of the turbine. It is seen from the figure that size of the said unit decreases with increase in pressure ratio as well as at higher TITs. However, the increased metal thickness at higher TITs may limit the economic advantages owing to reduced sizes.

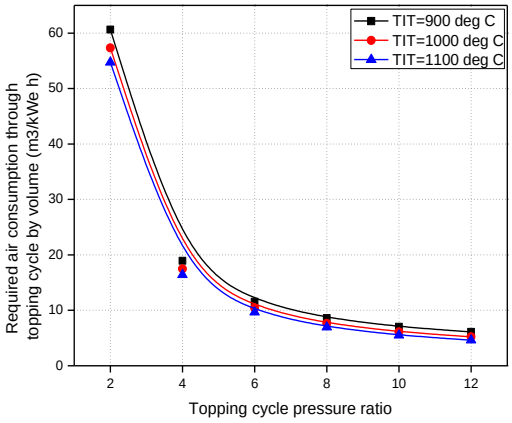

Figure 8. Variation in required air consumption through topping cycle by volume with topping cycle pressure ratio

The heat exchanger of the CHX unit is one of the most important and critical components used in the plant. A high pressure high temperature heat exchanger is required for this purpose and the design needs to be optimized from the sizing

and cost point of view. Also the design of the other heat exchangers used in the plant needs to be studied from the sizing point of view.

It is seen from "Fig. 2" that the plant is most efficient at about of r_p=6. The performance of the plant along with sizing of the heat exchangers used in the plant is shown in "Table 5", at different TITs. The size of the heat exchanger (UA) used in the CHX unit increases with increase in TIT.

Sizing of the heat exchanger of CHX unit increases with increase in gas turbine inlet temperature because of the log mean temperature difference (LMTD) decreases rapidly with increase in the same. Also the rate of heat transfer decreases with increase in gas turbine inlet temperature but the LMTD of the other heat exchangers increases or remain same. This ultimately effects the size of other heat exchangers to decrease with increase in gas turbine inlet temperature.

Component exergy losses for the plant components and the useful exergy of the plant with respect to fuel exergy (in percentage) is shown in "Fig. 9" at rp=4 and TIT=10000C. "Fig. 9" shows that the major exergy destruction takes place in the gasifier and the CHX unit, together accounting for about 42% of the total input.

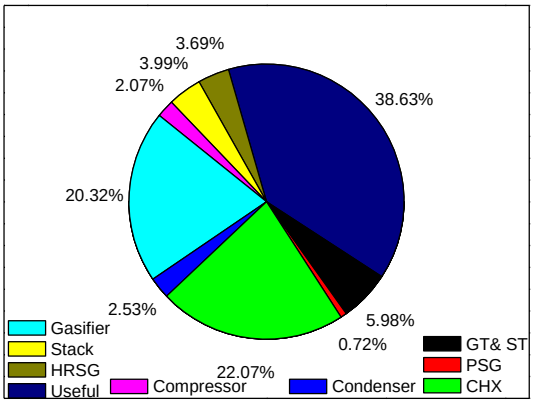

Figure 9. Component exergy loss and useful exergy of the plant at TIT=1000^{0}C and rp=4.

Exergy loss of the individual plant components with respect to fuel exergy (in kW) at optimal pressure ratios and at different TITs is shown in "Table 6".

It is seen form the "Table 6" that total exergy loss decreases with increase in gas turbine inlet temperature. This is because as the TIT increases required ESBC decreases which results in the loss of chemical exergy of the gasifier and combustor of the CHX unit to decrease. Also, at higher TIT exergy loss of the heat exchanger of the CHX unit and exergy loss of the gas turbine decreases. Among all the plant components gasfier, CHX unit and gas turbine are responsible for exergy destruction. This ultimately results in the exergy destruction decreases with increase in gas turbine inlet temperature.

Table 5. Performance of the plant and sizing of the heat exchangers at different operating conditions

	Scenario 1: r_p=6, TIT=900^{0}C				Scenario 2: r_p=6, TIT=1000^{0}C				Scenario 3: r_p=6, TIT=1100^{0}C			
Required Biomass Flow rate (kg/s)	0.0205				0.0185				0.0170			
Required Air Flow Rate (kg/s)	0.574				0.478				0.410			
Electrical Efficiency (%)	39.66				42.44				44.92			
FESR (%)	39.80				43.40				46.30			
Utility Steam Generation (kg/h)	193.60				162.75				140.61			
Sizing of the Heat Exchangers	ΔT_H (K)	ΔT_L (K)	Q_{tran} (kW)	UA (kW/K)	ΔT_H (K)	ΔT_L (K)	Q_{tran} (kW)	UA (kW/K)	ΔT_H (K)	ΔT_L (K)	Q_{tran} (kW)	UA (kW/K)
Heat exchanger	31.10	107.15	414.9	6.75	19.54	112.6	402.67	7.57	5.00	115.98	394.42	11.17
Superheater	7.80	151.74	17.75	0.37	13.31	156.57	15.33	0.263	16.62	159.48	13.46	0.213
Evaporator	151.74	15.0	91.05	1.54	156.57	15.00	79.32	1.31	159.48	15.0	69.97	1.14
Economizer	15.00	104.06	29.33	0.64	15.00	104.06	24.66	0.536	15.00	104.06	21.31	0.463
USG	38.65	95.00	19.47	0.31	38.65	95.0	16.37	0.26	38.65	95.0	14.14	0.23
Condenser	25.81	30.81	102.8	3.64	25.81	30.81	88.79	3.14	25.81	30.81	77.95	2.76

Table 6. Component exergy loss (in kW) at optimal pressure ratios and at different TITs

Component Name	TIT=900 degC	TIT=1000 degC	TIT=1100 degC
Gasifier	81	73.1	67.17
Combustor	65.39	52.98	44.09
Heat Exchanger	14.74	13.03	11.41
Compressor	10.08	8.4	7.21
Gas Tubine	24.52	21.34	19.07
Steam Turbine	3.68	3.18	2.79
Superheater	1.4	1.27	1.15
HP Evaporator	9.07	8.4	7.23
Economizer	2.18	1.9	1.68
Condenser	9.36	8.09	7.1
LP Evaporator	2.87	2.41	2.08
Stack	15.35	13.51	12.17
Total	239.64	207.61	183.15

Since the power cycle contains components like Gasifier and Combustor maximum exergy destruction takes place due the chemical reactions in the said units. Also significant amount of exergy destruction takes place in the heat exchanger of the CHX unit as well as in the gas turbine. It is seen from Fig.10 and Fig.11 that the plant is most efficient at topping cycle pressure ratio=6 and at gas turbine inlet temperature=1100 deg C considering preset assumed values of bottoming cycle parameters. However, some exergy can be recovered from the bottoming cycle by varying certain design parameter like steam turbine inlet temperature, inlet pressure along with the gas side economizer outlet temperature. The following section discusses the effect of the said parameters on the performance of the plant at optimized gas turbine pressure ratios and at corresponding gas turbine inlet temperatures.

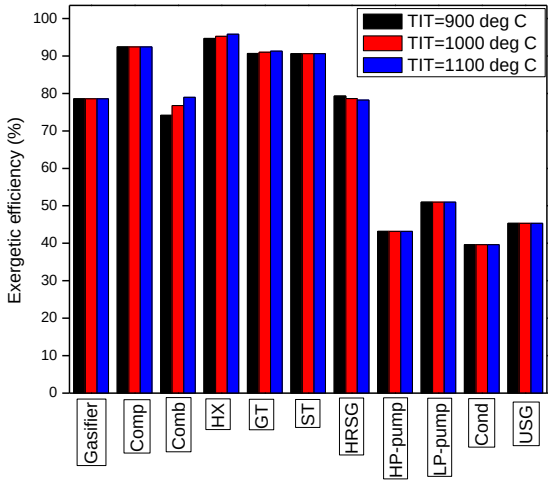

Figure 10. Variation in exergetic efficiency of the individual plant components at different GT TITs and at r_p=6

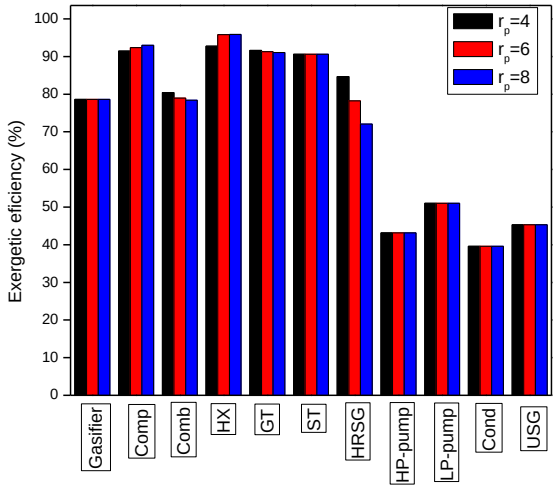

Figure 11. Variation in exergetic efficiency of the individual plant components at different pressure ratios and at GT TIT=1000 deg C

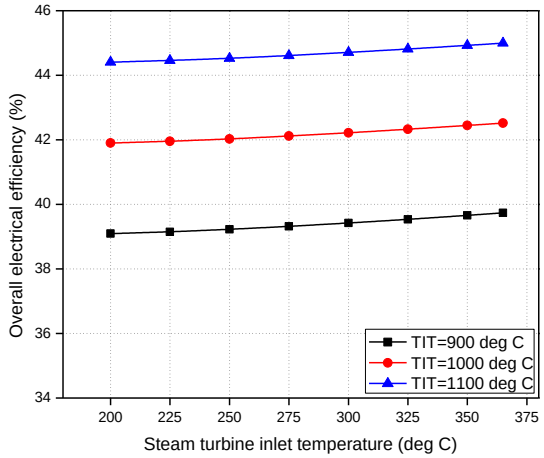

Figure 12. Variation in overall electrical efficiency of the plant with steam turbine inlet temperature

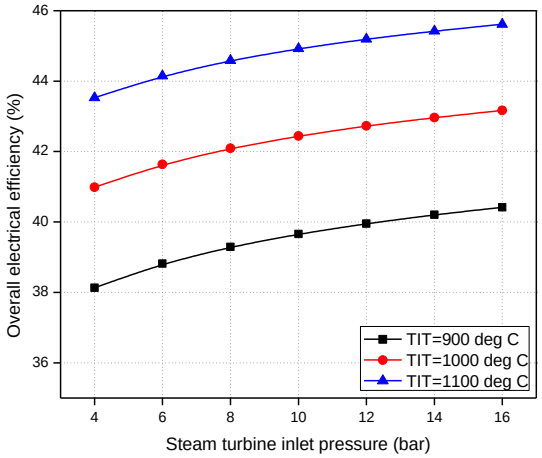

Figure 13. Variation in overall electrical efficiency of the plant with steam turbine inlet pressure

Variation in performance of the plant with variation in steam turbine inlet temperature and inlet pressure, considering gas side economizer outlet temperature is 1500C are shown in "Fig. 12" and "Fig. 13". It is clear from both the figures that increase in steam turbine inlet temperature and pressure increases the overall electrical efficiency of the plant. However, the inlet temperature and pressure must be within the plotted range to avoid the crossing of the temperature profiles. Variation in overall electrical efficiency and FESR with variation in gas side economizer outlet temperature considering steam turbine inlet temperature=350^{0}C and inlet pressure=10 bar is shown in "Fig. 14".

It is seen from "Fig. 14" that overall electrical efficiency decreases and FESR increases with increase in gas side economizer outlet temperature. This is due to the fact that as gas side economizer outlet temperature increases, the steam generation rate of the bottoming cycle decreases so the steam turbine output which ultimately results in the overall electrical efficiency of the plant to decrease. Also, increase in gas side economizer outlet temperature results in the increase in utility heat generation so in the FESR of the plant.

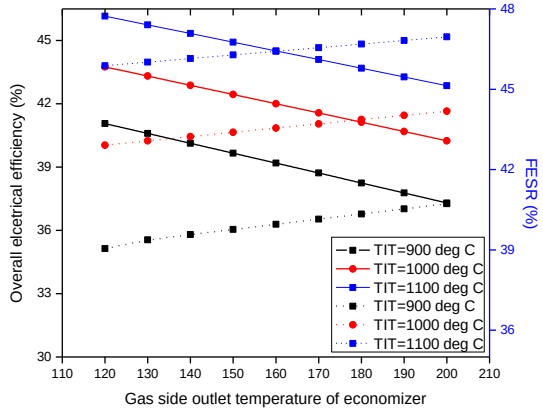

Figure 14. Variation in overall electrical efficiency and FESR of the plant with variation in gas side outlet temperature of the economizer.

5. Conclusion

Thermodynamic modeling and performance analyses along with the sizing of the plant components of a novel biomass based indirectly heated combined cogeneration plant is carried out in this paper. It is observed that the overall electrical efficiency of plant is maximized at some values of topping cycle pressure ratio, depending on the gas turbine inlet temperature. At a particular pressure ratio, the overall electrical efficiency of the plant increases with TIT. The ESBC decreases with increase in TITs and the value gets minimized at a particular value of topping cycle pressure ratio at respective TITs. The value of FESR is found to be optimized at particular pressure ratio and at higher TITs. In addition, it is found that the gas turbine pressure ratio and gas turbine inlet temperature influence the size of the plant components. Also the size of the CHX unit increases at higher TITs for any given value of pressure ratio. However, size of the other heat exchangers decreases with increase in GT TIT at any topping cycle pressure ratios.

From the Second Law analyses it is observed that maximum exergy destruction occurs in the combustor-heat exchanger duplex unit, followed by the gasifier. It can be concluded form the analyses that the plant can efficiently be operated at the pressure ratio 8 and at TIT=1100 deg C owing to the fact of increased size of CHX unit. Further, steam turbine inlet temperature and pressure, as well as, gas side exit temperature of economizer influence the performance of the plant. The maximized value of plant efficiency is about 45% at steam turbine inlet pressure 15 bar and inlet temperature 365 deg C.

In operational viewpoint of combined cogeneration plant the plant can be operated at topping cycle pressure ratio=6, GT TIT=1100 deg C and steam turbine inlet pressure=10 bar, inlet temperature=350 deg C and gas side

exit temperature of economizer, where the overall plant efficiency and FESR intersects each other.

Acknowledgements

The first author acknowledges the support provided by the Thermal Simulation and Computation (TSC) Lab at Mechanical Engineering Department of IIEST, Shibpur for carrying out the research work. The authors also acknowledge the cooperation of TU Delft (Delft University of Technology), The Netherlands, for providing the Cycle-Tempo software to the (TSC) lab, which has been used for the present study.

Appendix

Nomenclature

X_0: Mol of air for gasification, *mol of air/mol of biomass*

b: Moisture content of biomass, *mol of moisture/mol of biomass*

m: Mass flow rate of biomass, kg/s

c_p: Specific heat at constant pressure, *kJ/kg K*

w: Specific work, *kW/kg*

W: Total work, *kW*

T: Temperature, *K*

h^0: Specific enthalpy of formation, *kJ/kg*

$X_0^{'}$: Mol of air for combustion, *mol of air/mol of producer gas*

s: Specific entropy, *kJ/kg K*

X_j: j-th component in producer gas, *%*

X_k: k-th component in combustion air, *%*

X_m: m-th component in flue gas, *%*

X_{fg}: Total mol of flue gas, *mol*

X_s: Total mol of steam, *mol*

h: Specific steam enthalpy, kJ/kg

Q_U: Utility heat, *kW*

ΔF: Fuel energy savings, *kW*

e: Specific exergy, kW

e^{ch}: Specific chemical enthalpy, *kJ/kg*

$\overline{R}$: Universal gas constant, kJ/kg K

Greek Symbols

r_p =: Topping cycle pressure ratio

β: Multiplication factor

η_{gasi}: Gasification efficiency

η_G: Generator efficiency

η_P: Pump Efficiency

$\eta_{e,cc}$: Overall electrical efficiency

$\eta_{e,ref}$: Electrical efficiency of reference plant

$\eta_{b,ref}$: Heat efficiency of reference plant

$\eta_{exergetic}$: Exergetic efficiency

Abbreviation and Acronyms

i/in: Inlet

o/out: Outlet

CHX: Combustor-heat exchanger duplex unit

ECO: Economizer

ESBC: Electrical specific biomass consumption

EVAP: Evaporator

FESR: Fuel energy savings ratio

fg: Flue gas

GT: Gas turbines

LHV: Lower heating value

p.g: Producer gas

TIT: Turbine inlet temperature

USG/PSG: Utility/Process steam generator

ST: Steam turbine

SUP: Superheater

References

[1] B. Buragohain, P. Mahanta, and V.S. Moholkar, "Biomass gasification for decentralized power generation: The Indian perspective", Renewable and Sustainable Energy Reviews, Vol. 14, pp. 73-92, 2010. (Article) doi:10.1016/j.rser.2009.07.034

[2] Ankur Scientific Energy Technologies Pvt. Ltd. Website: http://www.ankurscientific.com/ (website)

[3] C. Syred, W. Fick, A. J. Griffiths, and N. Syred, "Cyclone gasifier and cycle combustor for the use of biomass derived gas in the operation of a small gas turbine in co-generation plant", Fuel, Vol. 83, pp. 2381-2392, 2000. (Article)

[4] A. Bhattacharya, D. Manna, B. Paul, and A Datta, "Biomass integrated gasification combined cycle power generation with supplementary biomass firing: Energy and exergy based performance analysis", Energy, Vol. 36, pp. 2599-2610, 2011. (Article) doi:10.1016/j.energy.2011.01.054

[5] Yap, and M. Roy, Biomass integrated gasification combined cycles (BIGCC), University of New Orleans Theses and Dissertations, Paper 206, 2004. (Report)

[6] N.S. Barman, S. Ghosh, and S. De, "Gasification of biomass in a fixed bed downdraft gasifier-A realistic model including tar", Bioresource Technology, Vol. 107, pp. 505-511, 2012. (Article) doi:10.1016/j.biortech.2011.12.124

[7] A. Datta, R. Ganguli, and L. Sarkar, "Energy and exergy analyses of an externally fired gas turbine (egft), cycle integrated with biomass gasifier for distributed power generation", Energy, Vol. 35, pp. 341-350, 2010. (Article)

[8] P. Mondal, and S. Ghosh, "Biomass based indirectly heated combined cycle plant: Energetic and exergetic performance analyses", International Journal of Innovative Research in Science, Engineering and Technology, Vol. 3, Issue 2, pp. 9285-9294, 2014. (Article)

[9] K.A. Al-attab, and Z.A. Zainal, "Performance of high-temperature heat exchangers in biomass fuel powered externally fired gas turbine systems", Renewable Energy, Vol. 35, pp. 913–920, 2010. (Article) doi:10.1016/j.renene.2009.11.038

[10] S. Soltani, S.M.S. Mahamoudi, M. Yari, and M.A. Rosen, "Thermodynamic analyses of an externally fired gas turbine combined cycle integrated with biomass gasification plant", Energy Conversion and Management, Vol. 70, pp. 107-115, 2013. (Article) doi:10.1016/j.enconman.2013.03.002

[11] Cycle-Tempo Software, Release 5 (TU Delft), 2012 (Available: http://www.cycle-tempo.nl/.) (Website)

[12] J. H. Horlock, Cogeneration-Combined Heat and Power (CHP), Pergamon Press, New York, 1987. (Book)

[13] S. Ghosh, and S. De, "First and second law performance variations of coal gasification fuel-cell based combined cogeneration plant with varying load", Proceedings of the Institution of Mechanical Engineers, Part A, Journal of Power and Energy, pp. 477-485, 2004. (Article)

[14] M. J Moran, "Availability Analysis: A Guide to Efficient Energy Use", Prentice-Hall, Englewood Cliffs, New Jersey, 1982 (Book)